Science of the Total Environment 409 (2011) 1095–1103

Contents lists available at ScienceDirect

Science of the Total Environment

journal homepage: www.elsevier.com/locate/scitotenv

Using artificial fluorescent particles as tracers of livestock wastes within an agricultural catchment

Steve J. Granger [a,*], Roland Bol [a], Jane M.B. Hawkins [a], Sue M. White [b], Pamela S. Naden [c], Gareth H. Old [c], Jon K. Marsh [d], Gary S. Bilotta [e], Richard E. Brazier [f], Christopher J.A. Macleod [a], Philip M. Haygarth [g]

[a] Soil, Water and Air Team, Sustainable Soils and Grassland Systems Department, Rothamsted Research, North Wyke, Okehampton, Devon, EX20 2SB, UK
[b] Natural Resources Department, Cranfield University, Cranfield, Bedfordshire, MK43 0AL, UK
[c] Centre for Ecology and Hydrology, Wallingford, Oxford, OX10 8BB, UK
[d] Environmental Tracing Systems Ltd, The Coach House, Bannachra, Helensburgh G84 9EF, UK
[e] School of Environment and Technology, University of Brighton, Brighton, BN2 4GJ, UK
[f] School of Geography, College of Life and Environmental Sciences, The University of Exeter, Amory Building, Rennes Drive, Exeter, Devon, EX4 4QJ, UK
[g] Lancaster Environment Centre, Lancaster University, Lancaster, LA1 4YQ, UK

ARTICLE INFO

Article history:
Received 31 August 2010
Received in revised form 29 November 2010
Accepted 1 December 2010
Available online 14 January 2011

Keywords:
Tracing
Particles
Animal waste
Agricultural catchments
Storm events

ABSTRACT

Evidence for the movement of agricultural slurry and associated pollutants into surface waters is often anecdotal, particularly with relation to its 'particulate' components which receive less attention than 'bio-available' soluble phases. To assess the extent of movement of slurry particles artificial fluorescent particles were mixed with slurry and applied to a field sub-catchment within a headwater catchment. Particles were 2–60 μm in diameter and two different densities, 2.7 and 1.2 g cm^{-3} representing 'inorganic' and 'organic' material. Water samples from the field and catchment outlet were collected during two storm events following slurry application and analysed for particle and suspended sediment concentrations (SSC). SSC from the field and catchment outlet always formed clockwise hysteresis loops indicating sediment exhaustion and particles of the two densities were always found to be positively correlated. Particles from the field formed clockwise hysteresis loops during the first discharge event after slurry application, but anti-clockwise hysteresis loops during the second monitored event which indicated a depletion of readily mobilisable particles. Particles from the catchment outlet always formed anticlockwise hysteresis loops. Particle size became finer spatially, between field and catchment outlet, and temporally, between successive storm events. The results indicate that slurry particles may be readily transported within catchments but that different areas may contribute to pollutant loads long after the main peak in SSC has passed. The density of the particles did not appear to have any effect on particle transport however the size of the particles may play a more important role in the 2–60 μm range.

1. Introduction

With the introduction of legislation and policy aimed at improving aquatic ecology and water quality in river basins (EEC, 2000) attention is increasingly focused on diffuse agricultural inputs of pollutants into surface waters and groundwater. In Europe and North America agricultural land often receives large quantities of agricultural amendments such as inorganic fertilizers or managed livestock wastes, which are applied as a means to improve plant production but, in the case of the latter, also as a means of disposal of a waste product.

Managed livestock wastes comprise both solid and liquid forms (termed farmyard manure (FYM) and slurry respectively) and in the United Kingdom it is estimated that some 78 million tonnes are produced annually needing storage and disposal (Smith and Chambers, 1993). Farmyard manure is typically a coarse, heterogeneous mix of dung, urine and bedding materials with high dry matter content while slurry has a lower dry matter content and is a more homogenous mix of dung, urine, some bedding and other surface washings and discharges (Chadwick and Chen, 2002). Both forms of livestock waste contain high levels of nutrients such as nitrogen (N) and phosphorus (P) as well as high organic contents (Chadwick and Chen, 2002) which can have a significant impact if released into aquatic environments. Therefore the application of these amendments to land has long been implicated by researchers as a source of diffuse pollution in aquatic systems (McDowell et al., 2007; McDowell and Sharpley, 2001; Smith et al., 2002; Smith et al., 1998). With the increased intensification of farming practices over the past 50 years (Chamberlain et al., 2000), stocking densities on grassland farms have generally increased, leading not only

* Corresponding author. Tel.: +44 1837 883500; fax: +44 1837 82139.
E-mail address: steve.granger@bbsrc.ac.uk (S.J. Granger).

0048-9697/$ – see front matter © 2010 Elsevier B.V. All rights reserved.
doi:10.1016/j.scitotenv.2010.12.005

to an increase in wastes applied to the land, but also the proportion which is stored and applied as slurry. Given the more aqueous nature of slurry and its smaller particle size compared with that of FYM, slurry components are potentially more mobile and at greater risk of loss from land to water. However, few studies actually provide evidence of a direct link between the slurry applied to land and the occurrence of pollutants in water bodies (Haygarth et al., 2006).

The pollutants within slurry can be broadly divided into two categories; those that are dissolved and those that are particulate, a division which is widely used in the literature particularly in relation to P (Granger et al., 2010a; Haygarth et al., 2005). While soluble pollutants are often the focus of experimental studies, as they are perceived to be the fraction that is most bio-available, the particulate fraction has received little attention (Granger et al., 2007). These slurry particles, of undetermined size and nature, may act as vectors to pollutants such as inorganic P and N as well as consisting of organic forms of those nutrients in their own right. The particles may also cause a high biological oxygen demand as the carbon within them is respired within aquatic environments (Defra, 2002) and they may act as vectors for micro-organisms leading to possible pathogenic contamination of water bodies (Droppo, 2001; Oliver et al., 2005). In an attempt to provide evidence for the movement of slurry particulates from land to drainage waters, Granger et al (2010b) undertook a proof-of-concept study by applying the novel tracing approach of using artificial fluorescent particles mixed with slurry which was then applied to 1 ha drained and undrained lysimeters. The particles, normally used in marine and freshwater aquatic environments (Marsh et al., 1991; Marsh et al., 1993; McComb and Black, 2005), comprise a polymer combined with a fluorescent dye manufactured with a density matched to that of the particles which are being mimicked. The particles were created with a density to match that of 'organic matter' and with a median particle size (D_{50}) of 12 μm. Granger et al (2010b) found that the tracer particles did move from the land surface in runoff leaving the lysimeters and particle numbers were found to change with discharge in a similar fashion to that of suspended sediment, namely concentrations increased on the rising limb of the hydrograph and decreased on the falling limb.

While this proof-of-concept study was successful in improving our understanding of the processes and pathways that slurry derived particles are subject to before their entrainment in drainage waters, there are aspects which remain uncertain. To address these uncertainties the tracer was used at a landscape scale in a small headwater catchment to better understand i) whether particles with differing densities were mobilised and transported, ii) if particles could be transported away from their point of field application to nearby surface waters, and iii) if the particle size affected particle transport.

2. Materials and methods

2.1. Study site

Located in Devon, SW England, the Den Brook catchment (50°46′N 3°52′W) is a first-order headwater catchment 48 ha in size (Fig. 1a and b), characterised by a slowly permeable seasonally waterlogged clay soil of the Hallsworth series (Harrod and Hogan, 2008) (Typic Haplaquept (USDA); stagnogley (UK); HOST Class 24). The catchment receives high levels of rainfall with an annual 40 year average of 1050 mm, the majority of which typically falls in the winter/spring (Armstrong and Garwood, 1991). The catchment has a limited amount of field drainage installed, predominantly draining areas close to the Den Brook. The heavy soil type and wet winter weather conditions cause the

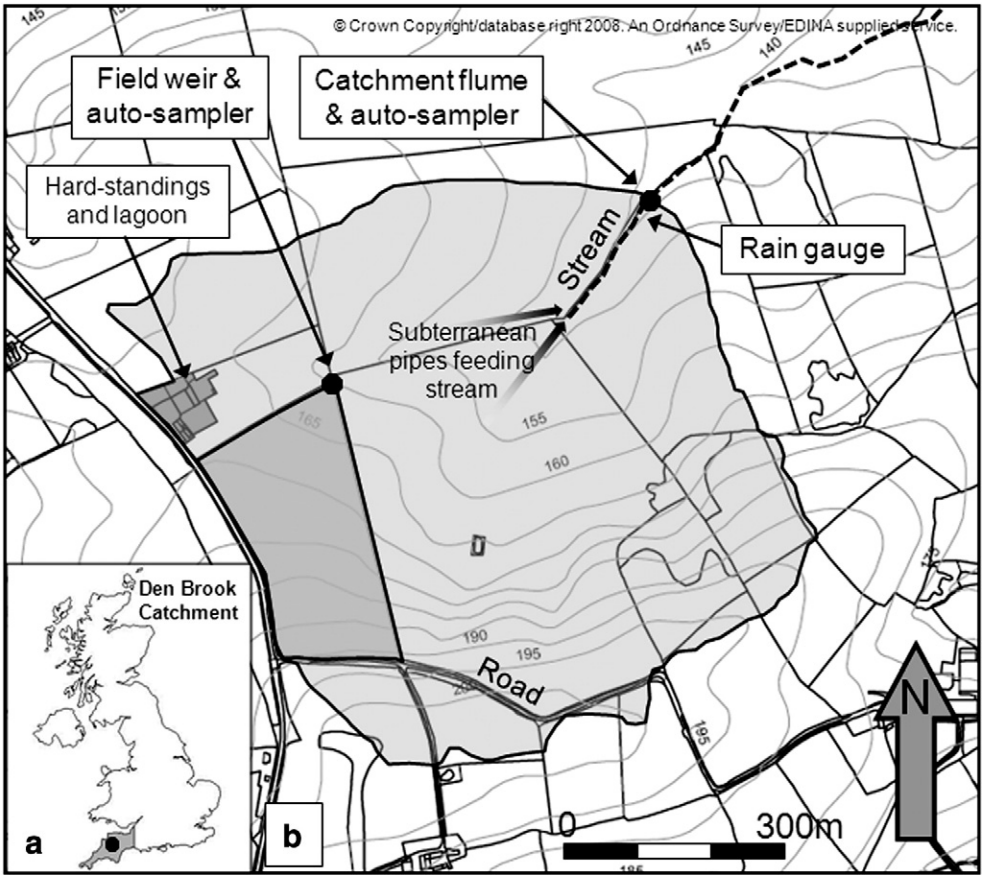

Fig. 1. Maps showing (a) the location of the Den Brook catchment within the south west UK. and (b) the Den Brook catchment boundary and the nested field sub-catchment and their associated sampling points.
[Reproduced with kind permission from Springer Science Business Media: Granger et al. (2010c), Fig. 1.].

hydrological response to rainfall to be very flashy with a large proportion of the response being saturation-excess overland flow (Armstrong and Garwood, 1991; Harris et al., 1984; Trafford and Rycroft, 1973). The catchment is predominantly managed as grassland grazed by cattle and sheep and the sward is dominated by perennial ryegrass receiving periodic applications of manure, inorganic fertilizer (N, P and K) and livestock excretal returns during the spring/summer. Within the catchment there is also a hard-standing (Fig. 1b) which comprises an area of concrete and animal housing that is served by a slurry lagoon receiving animal waste and contaminated farmyard run-off. This area is connected to the Den Brook by a large drainage pipe (Fig. 1b), which intermittently discharges farmyard run-off into the stream. The extent of this connection is poorly understood; however, in 2003 the slurry lagoon was rebuilt in an attempt to reduce pollution entering the stream. Waste contained within the lagoon is spread within the catchment area when ground conditions allow, typically during the spring/summer. To the south of the catchment, a drain delivers run-off from a road via a concrete conduit.

Within the catchment, a single field had been defined as a sub-catchment and was also monitored for flow. The field at the west of the catchment (Fig. 1b) represents 12% of the catchment area and slopes at about 5° from its SW to NE corner. The field is bounded on its upslope sides to the south and west by earth banks (approx 1 m high) while on its downslope sides only livestock fencing exists. However, on these sides, small earth banks (approx 15 cm high) have developed, possibly as a result of the field's recent history; it had been ploughed and used for maize production until 2006, when it was returned to grassland. The field, like the majority of the land within the catchment away from the stream channel, has no field drainage installed, and subsurface flow is considered to be negligible due to the low hydraulic conductivity of the subsoil (<10 mm day^{-1}) (Armstrong and Garwood, 1991). Due to the nature of the slope and the presence of surrounding banks, all surface runoff is concentrated towards the NE corner of the field.

2.2. Experimental design

2.2.1. Hydrological measurements

Discharge (Q) from the catchment was measured using a trapezoidal flume, which has been installed since 2001. Stage height, from which Q was calculated, was measured on 5-minute time-steps by a pressure transducer in a stilling well, 1 m upstream of the flume and was recorded by a data logger (Campbell Scientific CR10X). Discharge from the field sub-catchment was measured in the NE corner where a 45° 'V' notch weir was installed in 2006/07 and calibrated manually through the collection of over 100 measurements of Q at a range of stage heights. All surface flow occurring within the field was channelled down to the weir where an auto-sampler (ISCO 6712) was situated. Discharge was calculated from the stage height measured by the auto-sampler's integrated bubbler module within a stilling-well. Calibration of both the catchment outlet flume and the field weir enabled Q to be estimated using a rating curve with uncertainty bands by a technique developed by Krueger et al. (2010) based on estimates of the errors associated with its calibration (Bilotta et al., 2010). The mean Q line of this uncertainty interval has been used to give a clearer visual indication of the nature of the Q response. The values of Q cited, or parameters related to Q, are the mean value within the uncertainty interval.

Rainfall was recorded at the catchment outlet by a tipping-bucket rain gauge (Rain-wise Bar Harbor, ME), which recorded the total number of tips per minute (each tip equivalent to 0.254 mm rainfall).

2.2.2. Tracer design and application

Initial unpublished investigations into the density of <60 μm slurry material gave values higher than expected (1.7 to 1.8 g cm^{-3}) for a material assumed to largely comprised organic material (e.g. undigested grass, bedding materials, etc.). A loss of material on ignition at 550 °C indicated that approximately 30% of the slurry comprised inorganic particles. As a result of this, two different density particle tracers were created for the study and differentiated by colour: magenta particles to represent that of 'inorganic' material found in cattle slurry and yellow particles to represent organic material. It was decided that densities of 1.2 g cm^{-3} and 2.7 g cm^{-3} would be used for organic and inorganic particles respectively as this would give an overall total slurry density of 1.7 g cm^{-3} and would be realistic densities for these types of material (Skaven-Haug, 1972).

Slurry was applied to the field on the 6th and 7th of May 2008. The slurry was sourced from the slurry lagoon within the catchment, mixed and applied at a rate of 50 m^3 ha^{-1} via a traditional vacuum pump and splash plate spreader. As the slurry was pumped into the tanker under vacuum from the lagoon, equal measures of tracer particles were drawn into the tanker via a separate inlet valve to ensure mixing. The slurry was applied to 5 ha of the field, leaving a 10 m buffer around the edge of the field and excluding the area directly in front of the V-notch weir. The slurry tankers were calibrated so that it was known how many tankers were needed to cover the field at the required application rate. For both density particles, 90 kg of tracer was applied to the field in predetermined and equal fractions; hence each tanker had the same mass of tracer.

2.3. Sampling and analysis

The particle size distribution (PSD) of the raw tracer particles was measured using a LISST 100 laser diffraction particle size analyser (Sequoia Scientific, USA). In both cases, ten analyses of the pure tracer were undertaken and a mean result generated. The PSD by volume for the two different density particle tracers are presented in Fig. 2. Both tracers exhibited a bi-modal distribution with peaks in particles at 30–40 μm and

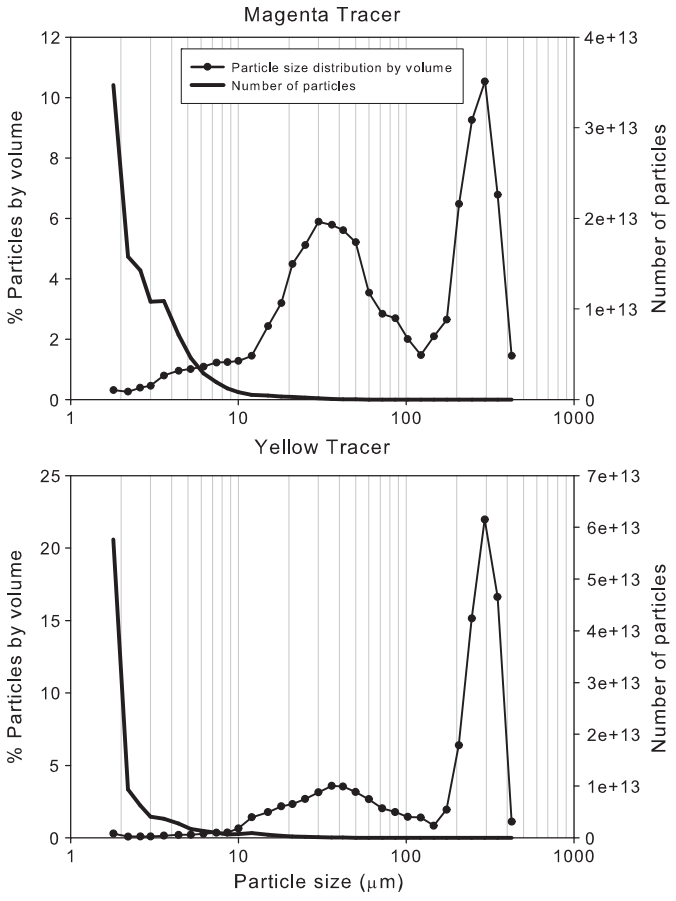

Fig. 2. The particle size distribution by volume and number for both magenta and yellow tracer particles.

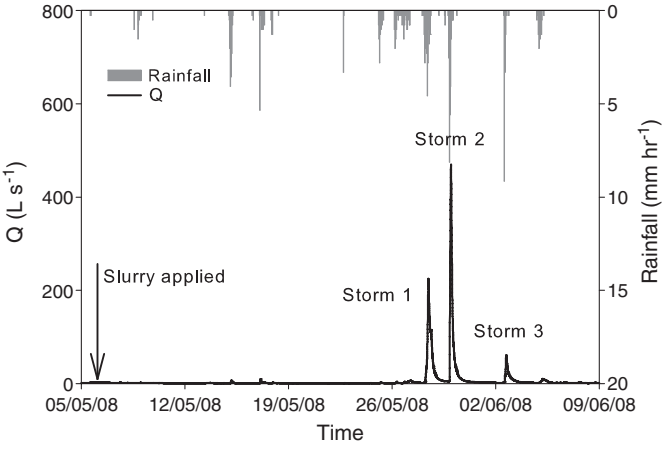

Fig. 3. The rainfall recorded in the Den Brook catchment and the hydrological response at the catchment outlet over the study period. The relative timing of the slurry application to the field sub-catchment and the three main storm events is indicated.

also at 300 μm. Assuming that the mean particle shape is spherical it is possible to calculate the volume of an individual particle at each PSD division. From the percentage by volume of tracer particles and the density of the material, the total number of particles can be calculated. The total numbers of magenta and yellow particles applied to the field were 1.07×10^{14} and 9.21×10^{13} respectively. For both tracer densities >99.9% of all particles were <60 μm in diameter. As previous study using this approach (Granger et al., 2010b) had indicated that <2 μm particles did not appear to be an important component of slurry thus, these particles were also excluded from this study. With these particles excluded, the total number of particles applied between 2 and 60 μm was 7.25×10^{13} and 3.45×10^{13} for magenta and yellow particles respectively. From the PSD data it is possible to calculate the number of particles within different fractions of the 2 to 60 μm range which accounts for >99% of all particles applied. These data shows that of the 2–60 μm magenta particles 98.9% were 2–20 μm, 1.0% were 20–40 μm and 0.1% were 40–60 μm, and that of the yellow particles 97.7% were 2–20 μm, 2.0% were 20–40 μm and 0.3% were 40–60 μm. Given that more magenta particles were applied to the field than yellow, the magenta data were adjusted by applying a correction factor of 0.476 to the magenta counts based on the number of 2 to 60 μm particles applied. Hereafter, all magenta data presented were adjusted unless otherwise stated.

After the slurry had been applied to the field, the auto-samplers were manually started shortly before a forecast storm event and programmed to sample on a fixed 30 min time-step. The internal clocks of the auto-samplers were synchronised to Greenwich Mean Time prior to sampling. Samples, of 1 L in volume, were collected from both sample points using automated pump samplers which had depth-integrated inlets. Samples were collected from the field within 24 h of the last sample to be taken. Sub-samples were taken from well-shaken auto-sampler bottles and sent to Environmental Tracing Systems Ltd for particle count analysis. The total particle counts were based on a 5 mL sub-sample of the sample which was then filtered through a 0.45 μm cellulose nitrate filter paper (Whatman). The filter paper was transferred to a labelled microscope slide and each slide was then analysed on a fluorescence microscope (Leica DM600B) with a camera (DFC310) using digital image process software (LAS Image Analysis; Leica Microsystems). The analysis was completely automated and particles within the set thresholds for colour were counted and a histogram produced for each slide in units of counts per 5 mL (cts 5 mL^{-1}). For selected samples particle size was determined by counting the number of pixels for each particle to determine the area and calculating an equivalent particle diameter. Particle size analysis was undertaken on the first 100 particles encountered on pre-selected slides. The calibration of the instrument is carried out routinely and automatically at the start of every session as per the instrument manual. Replicate analyses were carried out on 17% of the samples analysed. For the magenta particles the co-efficient of variation (CV%) was found to be 6.6% over a sample range of 3 to 1400 cts 5 mL^{-1}, for yellow particles the CV% was 9.2% over a sample range of 0 to 282 cts 5 mL^{-1}. Prior to the release of the tracer particles, 10 background samples had been collected from the catchment outlet at the site in order to determine whether there was any background fluorescence in the samples. Although some pale/weak fluorescent particles were present in the samples they did not interfere with the very much brighter fluorescent tracer particles. No detailed analyses of these weakly fluorescent particles were carried out as they were easily differentiated from the tracer fluorescence.

Suspended sediment concentration (SSC) was determined through vacuum filtration, and subsequent drying at 105 °C, of a known sample volume through a pre-weighed GF/F filter paper (Whatman), with particle size retention of 0.7 μm (UK Standing Committee of Analysts, 1980).

2.4. Statistical analysis

Simple correlations and ANOVA were carried out using GenStat v10.1 (VSN International Ltd) and data were graphically presented using SigmaPlot v10.0 (Systat Software Inc). Sample precision was assessed using a one-way ANOVA to remove between sample variation and from the remainder of the variation CV% was calculated over all the replicated samples.

3. Results

3.1. Hydrological response

Rainfall and Q from the catchment outlet are presented in Fig. 3 for the 5 weeks following slurry application. A summary of the data from both catchment outlet and the field sub-catchment outlet are contained within Table 1. The hydrological response of this site is typical of other clay soil sites both with and without mole drainage (Armstrong and Garwood, 1991; Harris et al., 1984; Trafford and Rycroft, 1973). Discharge responds rapidly to the onset of rainfall forming characteristically peaky hydrographs, especially where there is no drainage present. Three main rainfall driven flow events occurred after slurry

Table 1
Summary of the hydrological data recorded for the three discharge events monitored in the Den Brook catchment.

					Catchment		Field	
	Storm duration (h)	Max rainfall intensity (mm h^{-1})	Rainfall volume (mm)	Antecedent rainfall (48 h)	Peak Q (l s^{-1})	Volume (m^3)	Peak Q (l s^{-1})	Volume (m^3)
Storm 1 28th May 2010	15	4.6	23.9	15.5	225 [a](177–272)	5332 [b](4442–6221)	23 [a](20–26)	313 [b](276–350)
Storm 2 29th May 2010	9	8.1	23.6	25.1	470 [a](309–631)	6875 [b](5233–8516)	49 [a](41–56)	518 [b](446–590)
Storm 3 2nd June 2010	9	9.1	14.2	0	61 [a](52–70)	1132 [b](915–1349)	3 [a](3–4)	23 [b](16–29)

Values in parenthesis are the range of either [a]Q, or [b]volume, based on a rating curve with uncertainty bands by a technique developed by Krueger et al. (2010).

application during the monitored period. Storm 1 occurred 20 days after slurry application during the morning of the 28th May and lasted 15 h delivering 15 mm of rainfall with a maximum intensity of 5 mm h^{-1} (Fig. 4b). An estimation of the total storm Q (total event Q minus pre-storm base-flow) indicates that the runoff co-efficient was approximately 46%. The onset of Q from the field sub-catchment outlet occurred 2 h 30 min after the initial increase in catchment Q and peak Q was reached at the same time as peak Q at the catchment outlet.

Storm 2 occurred during the evening of the 29th May and although it delivered the same volume of rainfall as Storm 1 it was much more intense, lasting 9 h with a maximum intensity of 8 mm h^{-1}. It also fell on a catchment which had already received 25 mm of rainfall in the previous 48 h. The increased rainfall intensity coupled with the increased catchment wetness explains why in storm 2, the runoff co-efficient was 61%. The onset of Q from the field sub-catchment outlet started just 15 min after that of the catchment outlet and this reflects the high rainfall intensity coupled with the already wet nature of the soil leading to a rapid surface runoff response. Due to the unexpected nature of storm 2 auto-samplers were unfortunately not set in time to sample this event.

Storm 3 occurred during the afternoon of the 2nd June, 26 days after slurry application. This storm delivered the smallest volume of

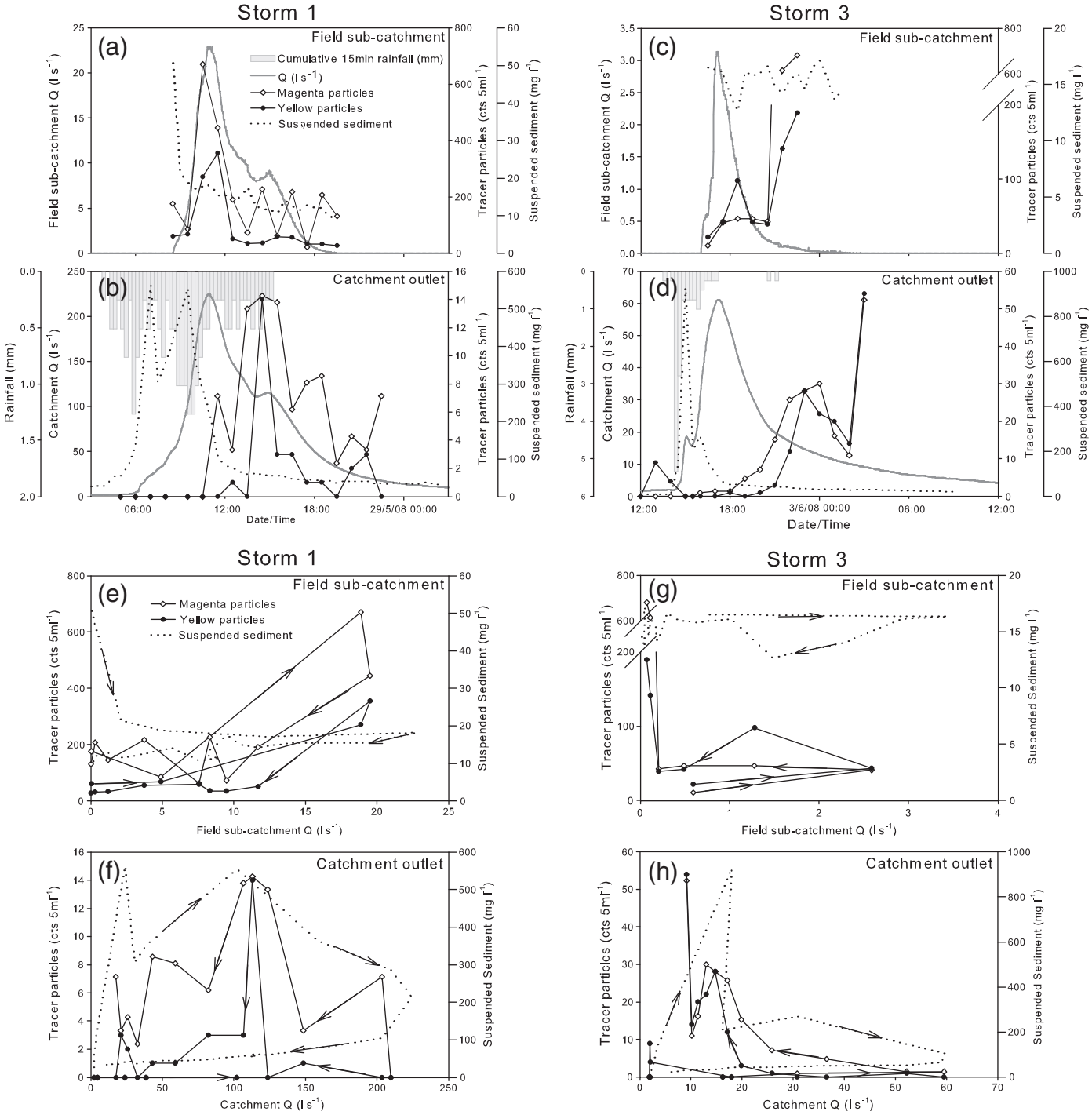

Fig. 4. Rainfall (grey bars) and discharge (▬) shown against numbers of yellow (•) and adjusted magenta (◇) tracer particles and suspended sediment concentration (▪▪▪▪▪▪) found in samples: storm 1 field sub-catchment (a) and catchment outlet (b), storm 3 field sub-catchment (c) and catchment outlet (d). Hysteresis loops for storm 1 field sub-catchment (f) and catchment outlet (f), storm 3 field sub-catchment (g) and catchment outlet (h) are also presented.

rainfall of the three main events with 15 mm; however it was the most intense monitored event lasting 9 h and at its peak producing 9 mm h^{-1} (Fig. 4d). The runoff co-efficient was just 17% and this low value has been attributed to the fact that the catchment was drying having had no rainfall in the preceding 48 h. Discharge at the catchment outlet increased almost immediately after rainfall had occurred. On the rising limb of the catchment outlet hydrograph a small subsidiary peak was observed after 45 min and this has been interpreted as rapid runoff from the hard-standings within the catchment due to the intense nature of the rainfall (Granger et al., 2010c). Discharge from the field sub-catchment outlet started 1 h 45 min after catchment Q had started to increase and peak Q again occurred at the same time as at the catchment outlet. The delay in the onset of Q between catchment and the field sub-catchment outlets when compared to storm 2 is explained by the lack of antecedent rainfall prior to storm 3 compared to storm 2.

3.2. Tracer particles and suspended solids in drainage from the field and catchment outlet

3.2.1. Storm 1

Tracer particles of both densities were present in the surface runoff from the field sub-catchment outlet from the very onset of sampling from Storm 1 (Fig. 4a). Sampling was initiated on a timed strategy and not triggered by Q. However, the first sample was taken almost immediately after Q had started to occur from the V-notch weir. The initial values from the field were therefore 176 and 61 cts 5 mL^{-1}, with nearly three times as many magenta particles in the sample than yellow. The peak in both tracer particle numbers occurred very close to that of the peak in Q. The highest number of magenta particles was 670 cts 5 mL^{-1} recorded just before peak Q while the highest number of yellow particles was 355 cts 5 mL^{-1} which occurred 30 min later when magenta counts were decreasing. In both cases the number of particles decreased rapidly after their peak had occurred although measured values of magenta particles fluctuated over most of the falling limb with values ranging between 22 and 227 cts 5 mL^{-1} but with no discernable trend. In contrast yellow particles did not exhibit much fluctuation in numbers over the falling limb with a range between 27 and 59 cts 5 mL^{-1}. Initially the SSC was 51 mg L^{-1} and occurred with the onset of runoff from the field sub-catchment outlet, but concentrations from this point fall, rapidly at first, throughout the duration of the hydrograph to 10 mg L^{-1}.

The number of tracer particles measured at the catchment outlet was considerably lower than those measured from the field sub-catchment and tracer particles were not recorded until sometime after Q had increased (Fig. 4b). Magenta and yellow particles were not present in samples at the catchment outlet until after peak Q had occurred and 3 to 4 h after they had been recorded leaving the field sub-catchment. The initial values of magenta and yellow particles were 7 and 1 cts 5 mL^{-1} and a peak in particle numbers of 14 cts 5 mL^{-1} for both magenta and yellow particles occurred 3 h 40 min after peak Q. The number of both types of particle generally declined over the rest of the falling limb of the hydrograph and ranged from 2 to 14 cts 5 mL^{-1} for magenta particles and 0 to 3 cts 5 mL^{-1} for yellow particles. Suspended sediment concentrations at the catchment outlet rose rapidly from 27 mg L^{-1} during base flow to form two peaks in concentrations of 562 and 555 mg L^{-1} before peak Q was reached. Concentrations then dropped rapidly before reaching a more slowly declining concentration just after peak Q had occurred almost reaching pre-storm concentrations of 32 mg L^{-1} 15 h 30 min after peak Q.

3.2.2. Storm 3

The numbers of both magenta and yellow particles were more comparable to each other during storm 3 compared with storm 1. The first sample was collected 30 min after the onset of Q from the field sub-catchment outlet and numbers increased rapidly on the rising limb of the hydrograph with both peaking 80 min after peak Q had occurred with values of 47 and 98 cts 5 mL^{-1} respectively (Fig. 4c). Yellow particle numbers rapidly fall back to 39 cts mL^{-1} over the following 60 min while magenta particle numbers fall only slightly to 43 cts 5 mL^{-1} over the same period; however, over the next 60 min numbers increase rapidly despite Q decreasing. Values of 614 and 680 cts 5 mL^{-1} for magenta particles were measured while yellow particles increased to 141 and 189 cts 5 mL^{-1} over the same period. Suspended sediment concentrations were low, ranging from 13 to 17 mg L^{-1}, and displayed no discernable trend over the duration of the hydrograph.

As was seen with Storm 1, the concentration of particles recorded at the catchment outlet reflected that of the field sub-catchment but with the peak in particle numbers occurring later than the peak in Q on the falling limb of the hydrograph (Fig. 4d). Numbers of magenta particles ranged between 0 and 1 cts 5 mL^{-1} until after peak catchment Q had occurred. The number of magenta particles then steadily increased to a maximum of 30 cts 5 mL^{-1} about 7 h after peak Q, before dropping rapidly back to 11 cts 5 mL^{-1} over the following 2 h. As with the field sub-catchment, numbers of magenta particles then increase unexpectedly in the last sample to be taken to a maximum of 52cts 5 mL^{-1}. The same pattern occurred in yellow particle numbers with low concentrations before peak Q (0 to 9 cts 5 mL^{-1}) and an increase in numbers occurring at a similar time to the magenta particles on the falling limb of the hydrograph reaching 28 cts 5 mL^{-1} before reducing to 14 cts 5 mL^{-1}. However, the last sample also contained a maximum of 54 cts 5 mL^{-1}. Suspended sediment concentrations rose rapidly from 9 mg L^{-1} during base flow to 925 mg L^{-1} on the rising limb of the hydrograph and were associated with a small subsidiary peak in Q. Concentrations, then fell rapidly back before peak Q was reached and had almost reached pre-event concentrations 15 h later.

3.3. Particle loads

Tracer particle loads were calculated for each monitored period using linear interpolation of original, unadjusted, point concentration data followed by multiplication with the mean Q within the uncertainty interval. The minimum and maximum loads, based on the uncertainty interval, are presented in parenthesis.

During storm 1, 4.17×10^{10} ($3.70–4.65\times10^{10}$) magenta particles and 1.01×10^{10} ($8.98\times10^{9}–1.13\times10^{10}$) yellow particles left the field sub-catchment with the highest flux of both associated with peak Q. This represents 0.05% of the magenta particles and 0.03% of the yellow particles initially applied to the field sub-catchment. Of these particles 1.15×10^{10} ($9.89\times10^{9}–1.31\times10^{10}$) magenta particles and 1.81×10^{9} ($1.57–2.05\times10^{9}$) yellow particles were monitored at the catchment outlet. These particles in turn represent 28% and 18% of the magenta and yellow particles that left the field sub-catchment. During storm 3, 4.70×10^{8} ($2.88–6.53\times10^{8}$) magenta particles and 2.23×10^{8} ($1.57–2.89\times10^{8}$) yellow particles were mobilised from the field sub-catchment representing just 0.0006% of the total magenta and yellow particles applied. From the catchment outlet 3.99×10^{9} ($2.81–5.77\times10^{9}$) magenta particles and 1.22×10^{9} ($7.99\times10^{8}–1.64\times10^{9}$) yellow particles were transported. The number of tracer particles leaving the catchment was greater than the number leaving the field sub-catchment during this event by factors of 8.5 and 5.5 for magenta and yellow particles respectively.

3.4. Tracer, suspended sediment and Q relationships

Tracer particle numbers of the two different densities were significantly positively correlated from the field sub-catchment ($r_{10}=0.83$; $p<0.001$) and catchment outlet ($r_{16}=0.55$; $p<0.05$) during storm 1 and both tracers along with SSC formed clockwise hysteresis loops (Fig. 4e). At the catchment outlet tracer particles

form anticlockwise hysteresis loops as their peak in concentration occurred after peak Q. However, SSC continued to form a clear clockwise hysteresis loop with a peak in concentration before peak Q (Fig. 4f). While the SSC peaks at the field sub-catchment and catchment outlets were found to be positively related ($r_{19} = 0.72$; $p < 0.001$), there was no relationship between tracer particle numbers at the two sampling locations with peaks from the field sub-catchment outlet occurring 4 h before the catchment outlet for magenta particles and 3 h for yellow particles.

During storm 3 magenta and yellow particles were again positively correlated from the field sub-catchment ($r_5 = 0.92$; $p < 0.01$) although this correlation is strongly influenced by the last two samples which had notably higher tracer particle numbers than were observed during the rest of the hydrograph. Without these two high value samples no significant relationship is present. The SSC continue to form a clockwise hysteresis loop. However, unlike storm 1, tracer particles form anticlockwise hysteresis loops (Fig. 4g). A significant correlation was again found at the catchment outlet between magenta and yellow particle numbers ($r_{15} = 0.92$; $p < 0.001$), both of which form anticlockwise hysteresis loops while the SSC continued to form a clockwise hysteresis loop (Fig. 4h). There continued to be a delay between field sub-catchment and catchment tracer particle peak numbers of between 4 and 5 h.

3.5. Tracer particle sizes

An assessment of tracer particle size was made on a limited number of samples collected to try to understand better the type of particles being transported and these data are presented in Table 2. Of the samples that were collected that contained tracer particles, at least 33% from each storm was analysed for particle sizes in 2–20, 20–40 and 40–60 μm size bands. Throughout both monitored storms, the vast majority of samples were 2–20 μm in size. The magenta particles were always 2–20 μm in size while a very limited number of larger yellow particles were found at the field sub-catchment outlet during storm 1. The yellow 20–60 μm particles comprised <1% of the particles counted although they comprised 2.3% of the original tracer. Given that the majority of tracer particles were in the 2–20 μm size band a further size analysis was undertaken on the sample that occurred at the main peak in tracer particle numbers looking at the 2–20 μm particles in more detail (Table 2). During storm 1 the majority of yellow and magenta particles found at the field sub-catchment outlet were 2–6 μm in diameter. Only 4% of magenta particles and 9% of yellow particles were 7–9 μm and just 2% and 5% were 10–20 μm. However, from the catchment outlet although the majority of tracer particles were still 2–6 μm, a greater percentage of 7–9 μm particles were present at peak Q (13% and 14% for magenta and yellow particles respectively) and no 10–20 μm particles were found present. A slightly different PSD was found during storm 3. From the field sub-catchment the majority of magenta and yellow particles were 2–6 μm in diameter with only 2% of magenta particles and 6% of magenta particles 7–10 μm and with just 1% of yellow particles and no magenta particles 10–20 μm. From the catchment outlet all tracer particles were in the 2–6 μm size range.

4. Discussion

The first storm after tracer particles were applied (Fig. 3) potentially reveals the most information about how organic and inorganic slurry derived materials move during rainfall events. Tracer particle response from the field sub-catchment occurred immediately Q was initiated (Fig. 4a) although this is perhaps unsurprising given that the majority of the land surface contributing to Q had received the slurry/particle mix. Peak tracer particle concentration corresponded with peak Q in a way typical of that of SSC reported in other studies (Granger et al., 2010c; Hejduk et al., 2006; Kronvang et al., 1997) and also initial trial studies using the fluorescent particles (Granger et al., 2010b). The hysteresis of the tracers of the two different densities and SSC were clockwise (Fig. 4e) and this common hysteresis is typically interpreted as a sediment exhaustion effect with surface runoff causing a flush of the smallest, most readily mobilised particles to be washed away (Hejduk et al., 2006; Lefrancois et al., 2007; Smith and Dragovich, 2009; Stutter et al., 2008). However, whereas SSC rapidly decline before peak Q is reached, both density tracer particles appear to peak with Q (Fig. 4a) and therefore their decline in numbers may be due to decline in Q rather than particle exhaustion. The density of the tracer particle appeared to make no difference to the way they responded with Q during both monitored storms at the field sub-catchment. However, the magenta particles were mobilised more readily than the yellow particles with 60% more of the magenta particle leaving the field sub-catchment than yellow particles. This is probably due to the magenta tracer being slightly less coarse than the yellow tracer given that the timing of the arrival of particle numbers at the field sub-catchment outlet was the same for both densities.

This pattern is again reflected at the catchment outlet, with tracer particle numbers strongly correlated between the two densities (Fig. 4b) , but with 28% of the magenta particles mobilised from the field sub-catchment actually making it to the catchment outlet compared to 18% of the yellow particles. As with SSC at the field sub-catchment outlet, SSC from the catchment outlet also produce a clockwise hysteresis loop (Fig. 4f). This may be attributed to the rapid remobilisation of in-channel sediment stores in conjunction with the rapid delivery of sediment from other readily mobilised sediment pools from within the catchment (Seeger et al., 2004; Smith and Dragovich, 2009) such as from the farm hard-standings (Granger et al., 2010c). However, hysteresis loops produced by the two density

Table 2
Details of samples analysed for tracer particle size and their particle size distribution.

	Particle size (μm)	Initial tracer		Storm 1				Storm 3			
				Field sub-catchment		Catchment outlet		Field sub-catchment		Catchment outlet	
Total number of samples	–	–		12		18		7		17	
Number of samples containing tracer particles	–	–		12		12		7		15	
Number of samples analysed for particle size	–	–		6		6		4		5	
Particle density (g cm^{-3})	–	2.7	1.2	2.7	1.2	2.7	1.2	2.7	1.2	2.7	1.2
[a] % particle size	2–20	98.9	97.7	100	99.1	100	100	100	100	100	100
	20–40	1.0	2.0	0	0.6	0	0	0	0	0	0
	40–60	0.1	0.3	0	0.3	0	0	0	0	0	0
Particles counted				100	100	30	14	98	98	59	28
[b] % particle size	2–6	93	87	94	86	87	86	98	93	100	100
	7–9	6	7	4	9	13	14	2	6	0	0
	10–20	2	6	2	5	0	0	0	1	0	0

[a] Analysis of particles within broad size ranges between 2 and 60 μm.
[b] Secondary more detailed analysis of particles found within the 2–20 μm size range.

tracer particles are anti-clockwise (Fig. 4f). Anti-clockwise hysteresis loops are less typical. When they occur they are interpreted as representing a change in sediment source such as channel bank collapse occurring on the hydrograph falling limb (Marttila and Kløve, 2010), the lack of available channel bed sediment at the start of the hydrograph (Lawler et al., 2006; Marttila and Kløve, 2010), the break up of armour layers and/or biofilms which can cause a delay of stored bed sediment mobilisation (Black et al., 2001; Lawler et al., 2006) or the contribution from a tributary that was late in supplying sediment from a distal sub-catchment (Lawler et al., 2006). In this case we know that the tracer particles have travelled from a distal sub-catchment and that organic and inorganic density particles from the field sub-catchment arrive at the catchment outlet 3–4 h after peak Q, which was about 5 h after peak SSC. Peaks in particle numbers between the field and catchment outlets were also offset by 3–4 h indicating the travel time for tracer particles over approximately 500 m. During storm 1 the 2–20 μm tracer particles were preferentially mobilised compared to 20–60 μm particles. However, within the 2–20 μm size range the distribution of particles sizes at peak Q was broadly similar to that of the original two tracers; the majority of the tracer particles being 2–6 μm, but with 7–10 μm and 10–20 μm fractions present (Table 2.). In contrast at the catchment outlet, when the peak in tracer particle numbers occurred, the size distribution had altered. Here, although 2–6 μm remained the most common particle size, more 7–10 μm particles were present and no 10–20 μm particles were found (Table 2.). This indicates that between the field sub-catchment and the catchment outlets some sorting of the tracer particles had occurred. Walling et al. (2000) found evidence of a pulse of coarse sediment on the rising limb of catchment hydrographs well before peak Q was reached and suggested that this may reflect the remobilisation of coarse sediment as flow velocity and shear stress increase, with finer sediment transported subsequently during the hydrograph peak and falling limb. Given the nature of the SSC response during storm 1 it might be assumed that on the falling limb of the hydrograph the contribution of sediment from across the catchment was falling, but from this data we can see that potentially slurry derived particles (and their associated pollutants) applied to the field were only just arriving. Therefore the SSC hysteresis loop at the catchment outlet is related not only to channel processes, but also to the timing, mixing and routing of water from different source regions within the catchment (Asselman, 1999).

The Q during storm 3 is far lower than during storm 1 (Fig. 3) however the SSC continue to form a clockwise hysteresis loop at the field sub-catchment (Fig. 4g). However, the particle tracer response during storm 3 is markedly different to that during storm 1 and this may be due to the effect of the large unmonitored rainfall event of storm 2. The numbers of the two tracer particle densities are broadly equal with the same percentage of the initial tracer leaving the field sub-catchment (Fig. 4c). The response of the tracer particles is less pronounced with Q than during storm 1 with only the yellow particles forming a clear peak in numbers, however both densities this time form anti-clockwise hysteresis loops (Fig. 4g). As it is unlikely that the field sub-catchment was significantly depleted of tracer particles, given that <0.04% of the total tracer particles applied were accounted for during storms 1 and 3 it is possible that storms 1 and 2 depleted the field of readily mobilisable particles within close proximity of the field sub-catchment outlet. The short but intense nature of the rainfall during storm 3, combined with low runoff, caused a delay in particles arriving at the field sub-catchment outlet as they were contributed from more distant regions of the field. However the precise nature of this mobilisation event is not fully understood as it is still surprising to see a large spike in tracer particle numbers at the end of the hydrograph (Fig. 4c). All tracer particles were 2–20 μm in size and both magenta and yellow tracers had a higher percentage of 2–6 μm diameter particles than either of the initial tracer or the tracer particles transported during storm 1 (Table 2.). However, given the vastly greater number of fine tracer particles to 'coarse' tracer particles it may be a function of the limited number of tracer particles assessed for size. It may also be caused by the size of event, given that in storm 3 Q is an order of magnitude lower than storm 1, and that the coarser tracer particles were simply not transported or were transported on the hydrograph rising limb (Walling et al., 2000).

The response from the catchment outlet is similar to that of storm 1. A clockwise hysteresis loop is formed by SSC while the main peak in tracer particle numbers occurs after peak Q forming anti-clockwise hysteresis loops (Fig. 4h). All the tracer particles assessed leaving the catchment outlet were in the 2–6 μm range again (Table 2) indicating a fining both spatially, between field sub-catchment and catchment outlets, and temporally between storms 1 and 3. However, during storm 3 a greater number of tracer particles were monitored leaving the catchment outlet than from the field sub-catchment. The interpretation of this is that storm 1 and the larger storm 2 mobilised a massive number of tracer particles causing the field to be broadly depleted of readily mobilised tracer particles. A large number of these tracer particles were deposited between the field sub-catchment and catchment outlets when storm 2 Q subsided, only to be remobilised during storm 3. What is interesting is that despite these tracer particles being present they are not mobilised with the immediate increase in Q from the catchment outlet and a lag time of about 3 h between field sub-catchment and catchment tracer particle peaks (Fig. 4c and d). This might reflect the fact that different parts of the catchment and different pathways respond at different times. In this scenario the rising limb of the catchment hydrograph is largely made up of rapidly responding runoff from areas close to the channel or areas with a rapid high hydrological connectivity to the channel. However these pathways are separate to the pathways that runoff from the field sub-catchment follow. For example, it has been interpreted that the initial flow on the rising limb of the hydrograph is probably sourced from the farm hard-standing within the catchment (Granger et al., 2010c). For this hard-standing Q to not cause a mobilisation of tracer particles outside the field, it must follow a pathway different to that of the field runoff. Yet it must enter the stream channel to cause the initial increase in catchment Q. This would imply that few or none of the tracer particles outside the field sub-catchment are deposited within the channel and that they are largely on the soil surface between the channel and the field. Tracer particles which did make it to the channel during storms 1 and 2 were not deposited, but immediately removed. Therefore at some point, Q between the field sub-catchment and channel was too low to transport tracer particles across the land, while Q in the channel remained sufficiently high to remove any tracer present.

5. Conclusions

Organic and inorganic density slurry derived particles have been shown capable of travelling some distance over land to surface water bodies and that particle size becomes finer temporally and spatially. While the density of the tracer particle does not appear to affect how the particle is mobilised and transported by surface runoff the size of particle does appear to influence the numbers lost particularly when <60 μm. Tracer particles applied to the field sub-catchment arrived at the catchment outlet late on the hydrograph after SSC and Q peaks forming anticlockwise hysteresis loops. Therefore, slurry particles may be contributing to pollutant loads even when SSC are returning to background levels.

Once mobilised, both organic and inorganic density tracer particles may be redeposited elsewhere within the catchment ready for mobilisation with the next significant Q event. Although this study has indicated that while the Q of the overland flow may drop below levels sufficient to transport particles, the Q in the channel remains high enough to continue tracer particle transport, thus ensuring no deposition within the channel.

This tracing approach would appear to be useful in developing a better understanding of the timing and pathways of different particulate contributing areas within a catchment. Further work would need to look at PSD by number more closely and undertake tracer particle size analysis more closely and across the hydrograph to enable a very accurate determination of the PSD by number of the actual tracer released and the particles monitored.

Acknowledgements

This paper arises from research funded by Defra and was carried out under project PE0120. Rothamsted Research is supported by BBSRC. We acknowledge the help of Tobias Krueger (University of East Anglia), Jim Freer (University of Bristol), John Quinton (Lancaster University), Fraser Taylor (Environmental Tracing Systems Ltd) and the two anonymous reviewers for their constructive comments.

References

Armstrong AC, Garwood EA. Hydrological consequences of artificial drainage of grassland. Hydrol Process 1991;5:157–74.
Asselman NEM. Suspended sediment dynamics in a large drainage basin: the River Rhine. Hydrol Process 1999;13:1437–50.
Bilotta GS, Krueger T, Brazier RE, Butler P, Freer J, Hawkins JMB, et al. Assessing catchment-scale erosion and yields of suspended solids from improved temperate grassland. J Environ Monit 2010;12:731–9.
Black KS, Sun HY, Craig G, Paterson DM, Watson J, Tolhurst T. Incipient erosion of biostabilized sediments examined using particle-field optical holography. Environ Sci Technol 2001;35:2275–81.
Chadwick DR, Chen S. Manures. In: Haygarth PM, Jarvis SC, editors. Agriculture, Hydrology and Water Quality. CABI Publishing; 2002. p. 57–82.
Chamberlain DE, Fuller RJ, Bunce RGH, Duckworth JC, Shrubb M. Changes in the abundance of farmland birds in relation to the timing of agricultural intensification in England and Wales. J Appl Ecol 2000;37:771–88.
Defra. Code of Good Agricultural Practice for the Protection of Water. London: Defra Publications; 2002.
Droppo IG. Rethinking what constitutes suspended sediment. Hydrol Process 2001;15: 1551–64.
EEC. Directive 2000/60/EC of the European parliment and the council of 23 October 2000 establishing a framework for community action in the field of water policy. Off J Eur Commiunties 2000;L327:1-72.
Granger SJ, Bol R, Butler P, Haygarth PM, Naden P, Old G, et al. Processes affecting transfer of sediment and colloids, with associated phosphorus, from intensively farmed grasslands: tracing sediment and organic matter. Hydrol Process 2007;21: 417–22.
Granger SJ, Bol R, Anthony S, Owens PN, White SM, Haygarth PM. Towards a holistic classification of diffuse agricultural water pollution from intensively managed grasslands on heavy soils. Adv Agron 2010a;105:83-115.
Granger SJ, Bol R, Dixon L, Naden PS, Old GH, Marsh JK, et al. Assessing multiple novel tracers to improve the understanding of the contribution of agricultural farm waste to diffuse water pollution. J Environ Monit 2010b;12:1159–69.
Granger SJ, Hawkins JMB, Bol R, White SM, Naden P, Old G, et al. High temporal resolution monitoring of multiple pollutant responses in drainage from an intensively managed grassland catchment caused by a summer storm. Water Air Soil Pollut 2010c;205:377–93.
Harris GL, Goss MJ, Dowdell RJ, Howse KR, Morgan P. A study of mole drainage with simplified cultivation for autumn sown crops on a clay soil.2. Soil-water regimes, water balances and nutrient loss in drain water, 1978–80. J Agric Sci 1984;102: 561–81.
Harrod TR, Hogan DV. The soils of North Wyke and Rowden. Unpublished report to North Wyke Research, revised edition of original report by T.R. Harrod, Soil Survey of England and Wales (1981). Okehampton, Devon: North Wyke Research; 2008.
Haygarth PM, Condron LM, Heathwaite AL, Turner BL, Harris GP. The phosphorus transfer continuum: linking source to impact with an interdisciplinary and multi-scaled approach. Sci Total Environ 2005;344:5-14.
Haygarth PM, Bilotta GS, Bol R, Brazier RE, Butler PJ, Freer J, et al. Processes affecting transfer of sediment and colloids, with associated phosphorus, from intensively farmed grasslands: an overview of key issues. Hydrol Process 2006;20:4407–13.
Hejduk L, Hejduk A, Banasik K. Suspended Sediment Transport during Rainfall and Snowmelt-rainfall Floods in a Small Lowland Catchment, Central Poland. Wallingford UK: Cabi; 2006.
Kronvang B, Laubel A, Grant R. Suspended sediment and particulate phosphorus transport and delivery pathways in an arable catchment, Gelbæk Stream, Denmark. Hydrol Process 1997;11:627–42.
Krueger T, Freer J, Quinton JN, Macleod CJA, Bilotta GS, Brazier RE, et al. Ensemble evaluation of hydrological model hypotheses. Water Resour Res 2010;46.
Lawler DM, Petts GE, Foster IDL, Harper S. Turbidity dynamics during spring storm events in an urban headwater river system: the Upper Tame, West Midlands, UK. Sci Total Environ 2006;360:109–26.
Lefrancois J, Grimaldi C, Gascuel-Odoux C, Gilliet N. Suspended sediment and discharge relationships to identify bank degradation as a main sediment source on small agricultural catchments. Hydrol Process 2007;21:2923–33.
Marsh JK, Bale AJ, Uncles RJ, Dyer KR. A tracer technique for the study of suspended sediment dynamics in aquatic environments. Proceedings of the International Symposium on the Transport of Suspended Sediments and its Mathematical Modelling. International Association of Hydraulic Research, Florence, Italy, 2–5 September; 1991. p. 665–81.
Marsh JK, Bale AJ, Uncles RJ, Dyer KR. Particle tracing experiment in a small shallow lake: Loe Pool, UK. In: McManus J, Duck RW, editors. Geomorphology and Sedimentology of Lakes and Reservoirs. Chichester: John Wiley and Sons Ltd; 1993. p. 139–53.
Marttila H, Kløve B. Dynamics of erosion and suspended sediment transport from drained peatland forestry. J Hydrol 2010;388:414–25.
McComb P, Black K. Detailed observations of littoral transport using artificial sediment tracer, in a high-energy, rocky reef and iron sand environment. J Coast Res 2005;21: 358–73.
McDowell RW, Sharpley AN. Phosphorus losses in subsurface flow before and after manure application to intensively farmed land. Sci Total Environ 2001;278:113–25.
McDowell RW, Nash DM, Robertson F. Sources of phosphorus lost from a grazed pasture receiving simulated rainfall. J Environ Qual 2007;36:1281–8.
Oliver DM, Clegg CD, Haygarth PM, Heathwaite AL. Assessing the potential for pathogen transfer from grassland soils to surface waters. Advances in Agronomy, Vol 85. 85. San Diego: Elsevier Academic Press Inc; 2005. p. 125–80.
Seeger M, Errea MP, Begueria S, Arnaez J, Marti C, Garcia-Ruiz JM. Catchment soil moisture and rainfall characteristics as determinant factors for discharge/ suspended sediment hysteretic loops in a small headwater catchment in the Spanish Pyrenees. J Hydrol 2004;288:299–311.
Skaven-Haug SV. Volumetric relations in soil materials. 4th International Peat Congress, Espoo, Finland; 1972.
Smith KA, Chambers BJ. Utilizing the nitrogen content of organic manures on farms — problems and practical solutions. Soil Use Manage 1993;9:105–12.
Smith HG, Dragovich D. Interpreting sediment delivery processes using suspended sediment-discharge hysteresis patterns from nested upland catchments, south-eastern Australia. Hydrol Process 2009;23:2415–26.
Smith KA, Chalmers AG, Chambers BJ, Christie P. Organic manure phosphorus accumulation, mobility and management. Soil Use Manage 1998;14:154–9.
Smith KA, Beckwith CP, Chalmers AG, Jackson DR. Nitrate leaching following autumn and winter application of animal manures to grassland. Soil Use Manage 2002;18: 428–34.
Stutter MI, Langan SJ, Cooper RJ. Spatial contributions of diffuse inputs and within-channel processes to the form of stream water phosphorus over storm events. J Hydrol 2008;350:203–14.
Trafford BD, Rycroft DW. Observations on soil-water regimes in a drained clay soil. J Soil Sci 1973;24:380–91.
UK Standing Committee of Analysts. Suspended, settleable and total dissolved solids in waters and effluents. London: HMSO; 1980.
Walling DE, Owens PN, Waterfall BD, Leeks GJL, Wass PD. The particle size characteristics of fluvial suspended sediment in the Humber and Tweed catchments, UK. Sci Total Environ 2000;251:205–22.